

## Large-Scale Supramolecular Structure in Solutions of Low Molar Mass Compounds and Mixtures of Liquids: II. Kinetics of the Formation and Long-Time Stability

Marián Sedlák\*

*Institute of Experimental Physics, Slovak Academy of Sciences, Watsonova 47, 043 53 Košice, Slovakia*

*Received: November 29, 2005*

Kinetics of the formation of large-scale supramolecular structure and its long-time stability were investigated in detail in solutions of electrolytes, nonelectrolytes, and mixtures of liquids. This structure comprises submicron-sized domains (large clusters) with higher solute concentration than in the rest of solution. In the case of mixtures of liquids, a complete real-time monitoring of the structure formation was possible in all cases. In the case of solutions of solid samples, the observation was possible in cases when the structure formation was significantly slower than the dissolution process. The time scale on which the supramolecular structure develops varies from minutes to weeks, depending on the concrete system. The long-time stability of the developed structure was investigated in time intervals ranging up to 15 months. In some systems the resulting domain structure appears stable, in others a very slow ceasing of domains is observed over very long time intervals. In all cases, however, slow kinetic effects are present in the systems investigated. Among others, data on some common substances of great chemical and biological importance such as sodium chloride, acetic acid, glucose, and ethanol, are presented.

### Introduction

In the previous paper<sup>1</sup> of this series, a large-scale supramolecular structure in solutions of electrolytes, nonelectrolytes, and mixtures of liquids was described on the basis of extensive static and dynamic laser light scattering experiments. It was shown that solutes are distributed inhomogeneously on large length scales. Regions of higher and lower solute concentration exist in solution and give sufficient scattering contrast for experimental observation. These regions can be characterized as close-to-spherical discrete domains of higher solute density in a less dense rest of solution. These domains do contain solvent inside and can be characterized as loose associates (large clusters, aggregates). Their size distributions are usually significantly broad, ranging up to several hundreds of nanometers. Characteristic sizes of these inhomogeneities thus exceed angstrom dimensions of individual molecules by several orders of magnitude. The number of solute molecules per domain varies approximately in the range  $10^3$ – $10^8$ . The presence of supramolecular domains is reflected in light scattering data as a separate diffusive mode with diffusion coefficient  $D_s$ , which is relatively low (slow diffusion). The scattering amplitude of this mode  $A_s$  (contribution of domains to the overall scattering intensity) is strongly dependent on angle. Size distributions of domains are calculated from shapes of angular dependencies  $A_s(\theta)$ . Structural information obtained from static light scattering data correlates well with dynamic data calculated from  $D_s$ .

This paper deals with the kinetics of the supramolecular domain formation as well as with the long-time stability of these structures. Several types of kinetic effects will be described and evidenced by results obtained on various systems from the three classes discussed, i.e., solutions of electrolytes, nonelectrolytes, and mixtures of liquids.

### Experimental Section

Chemicals used for experiments were of analytical grade (mostly from Merck, Darmstadt). The following substances were used in this work: D-glucose, NaCl, Na<sub>2</sub>SO<sub>3</sub>, MgSO<sub>4</sub>, Al(NO<sub>3</sub>)<sub>3</sub>, acetic acid, dimethyl sulfoxide, ethanol, and benzene. Water was freshly double-distilled in a quartz apparatus and subsequently deionized by analytical grade mixed-bed ion-exchange resins (Bio-Rad, Richmond, CA). The resistivity of water was above 15 M $\Omega$  cm. Mixtures of liquids were prepared for kinetic measurements simply by dropping both liquids via 0.2  $\mu$ m filters directly into a scattering cell and gently shaking to allow for mixing. All liquids were easily miscible with very rapid mixing of components at the molecular level. This allowed to monitor the formation of supramolecular structures almost from the very beginning of this process. Intensive stirring of mixtures at various speeds for longer periods of time did not have any influence on data (just disabled to monitor the earliest stages of the process). All solid samples had to be stirred, of course, and then after dissolution allowed to stand before measurements for at least half an hour. The full dissolution was assured not only macroscopically by visual observation, but also by vapor pressure osmometry, which is sensitive to the concentration of free (i.e. “dissolved”) ions or molecules in solution. Measurements of osmotic pressure were performed by K-7000 vapor pressure osmometer (Knauer, Berlin). Long-time kinetics measurements were performed at  $T = 25$  °C. Temperature annealing and/or measurement at higher temperatures (various temperatures up to  $T = 80$  °C) did not have any measurable influence on the supramolecular structures, including such viscous system as the glycerol/water mixture.

The static light scattering (SLS) and dynamic light scattering (DLS) measurements were made using a Stabilite 2017–04S argon laser (Spectra Physics, Mountain View, CA) with 514.5 nm vertically polarized beam. Laser power was limited to 300 mW. No change of data with laser power was observed in this

\* E-mail: marsed@saske.sk.

range. A laboratory made goniometer with angular range from 30° to 150° was used to collect data for both static and dynamic light scattering experiments. The scattering cell was thermostated at 25 °C with a precision of  $\pm 0.1$  °C. Scattering intensities were measured by photon counting and normalized using a doubly distilled and filtered benzene as a standard. Solvent scattering was subtracted from solution scattering to obtain excess scattering intensities. In the case of mixtures of liquids, the excess scattering was taken as a contribution of compositional fluctuations to total scattering (anisotropic scattering and scattering due to density fluctuations were subtracted from the total scattering). Great attention was paid to the purity of samples necessary for work with weakly scattering systems.<sup>2–7</sup> Scattering cells were thoroughly cleaned from dust. All liquids were filtered through 0.2  $\mu\text{m}$  filters for the same reason. Solutions were centrifuged for 10 min at 5000 g. This very gentle centrifugation had no effect on samples but was able to eliminate some remaining dust residuals. Experiments on blank samples (non-structured mixtures or pure liquids) showed a complete dust removal (correct absolute values of scattering intensity without upturns in scattering intensity tracks, flat angular dependencies, as well as flat correlation curve baselines). Samples were centrifuged in a microchip-controlled centrifuge Jouan KR22i (Jouan, France). This centrifuge enables to set very precisely not only the relative centrifugal force (RCF) and centrifugation time (CT) but also the acceleration and braking by definition of the integral of the dependence of RCF on time. This allows exactly and reproducibly apply gravitational forces. Temperature was controlled by cooling and was set to  $T = 25$  °C. An ALV5000 correlator with a fast correlation board option and an ALV800 transputer board (ALV, Langen, Germany) were used for photon correlation measurements. Characteristic decay times of dynamic modes  $\tau_i$  and their relative amplitudes  $A_i(\tau_i)$  were evaluated through the moments of distribution functions of decay times  $A(\tau)$  obtained by fitting correlation curves using CONTIN<sup>8</sup> and GENDIST<sup>9,10</sup> programs as

$$g^{(1)}(t) = \int_0^\infty A(\tau) e^{-t/\tau} d\tau \quad (1)$$

Diffusion coefficients were calculated as  $D_i = (1/\tau_i)q^{-2}$ , where  $q$  is the scattering vector defined as  $q = (4\pi n/\lambda_0) \sin(\theta/2)$ , with  $n$  the solution refractive index,  $\lambda_0$  the laser wavelength, and  $\theta$  the scattering angle. Two diffusive modes were detected. They were characterized by diffusion coefficients  $D_f$ ,  $D_s$ , and amplitudes  $A_f$ ,  $A_s$  (subscripts f and s refer to faster and slower, respectively). Correlation curves at various angles were recorded concurrently with integral scattering intensities  $I(\theta)$  (solution excess scattering) and  $I_B(\theta)$  (scattering of a benzene standard). Normalized excess scattering amplitudes of the two dynamic modes  $A_f(\theta)$  and  $A_s(\theta)$  were calculated as

$$A_s(\theta) = \frac{I(\theta)/I_B(\theta)}{1 + A_f(\theta)/A_s(\theta)} \quad (2)$$

$$A_f(\theta) = \frac{I(\theta)/I_B(\theta)}{1 + A_s(\theta)/A_f(\theta)} \quad (3)$$

assuming that  $I(\theta)/I_B(\theta) = A_f(\theta) + A_s(\theta)$ . Dimensionless ratios  $A_s(\theta)/A_f(\theta)$  and  $A_f(\theta)/A_s(\theta)$  were taken from DLS spectra of relaxation times.

Angular dependencies of scattering intensity were usually measured several times on one sample and subsequently averaged. An optimized regularization technique (ORT)<sup>11,12</sup> was used for the calculation of domain size distributions from static

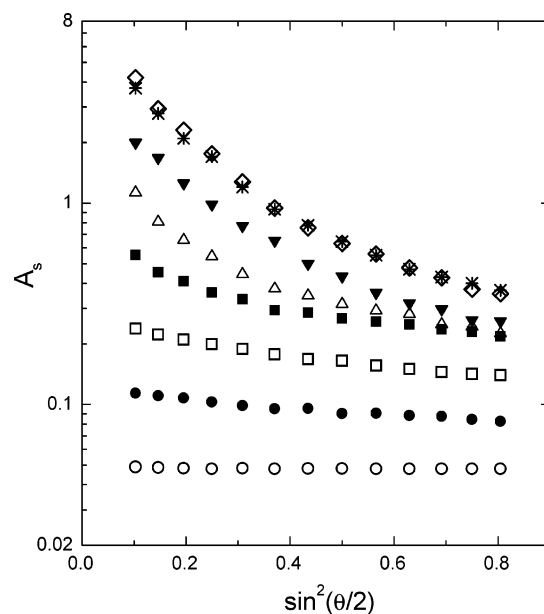


**Figure 1.** Kinetics of the cluster formation in the mixture of dimethyl sulfoxide and water (10.5 mass % of DMSO). Angular dependencies of scattering from clusters were taken 2 min ( $\circ$ ), 50 min ( $\bullet$ ), 4 h ( $\square$ ), 7 days ( $\blacksquare$ ), 11 days ( $\triangle$ ), 27 days ( $\blacktriangle$ ), 47 days ( $*$ ), and 260 days ( $\diamond$ ) after mixing. Clusters mean domains with different local solute concentration (local mixture composition) with respect to the rest of the sample and can be characterized as close-to-spherical polydisperse objects.<sup>1</sup>

light scattering data. The inversion of Fredholm integral equations of the first kind in optical sizing, which is an ill-posed problem from the mathematical point of view, is overcome in this case by the regularization technique. The size distribution function is searched as a linear combination of cubic B splines  $\phi_i(R)$  in a window delimited by  $R_{\min}$  and  $R_{\max}$

$$D(R) = \sum_{i=1}^n c_i \phi_i(R) \quad (4)$$

where the natural limits  $2R_{\min} = \pi/q_{\max}$  and  $2R_{\max} = \pi/q_{\min}$  may be exceeded to certain extent<sup>11,12</sup> ( $q_{\max}$  and  $q_{\min}$  are the maximum and minimum experimentally available scattering vectors). Scattering intensity is expressed via coefficients  $c_i$ , which are the unknowns that can be determined by a constrained least-squares condition. In our particular case, the amplitude of the slower mode  $A_s$  calculated by eq 2 (scattering contribution from domains) was used as the input scattering intensity for the ORT calculation of domain size distributions. The relative refractive index of particles with respect to solvent, which comes into calculation, is, in our case, an unknown parameter since the scattering contrast of domains is not exactly known. However, very similar results are obtained irrespective of concrete values of refractive index used in the calculation.

## Results and Discussion

Figures 1 and 2 show kinetics of the domain formation in the mixture of dimethyl sulfoxide and water (10.5 mass % of DMSO). The growth of domains is reflected in static light scattering (SLS) data by a continuous increase of the absolute value of the scattering contribution from domains  $A_s$  to the overall scattering and by increase of the slope of angular dependencies of  $A_s$ . The developing curvature in angular dependencies reflects the increasing polydispersity of domain sizes.<sup>1</sup> The growth of domains is reflected also in hydrodynamic

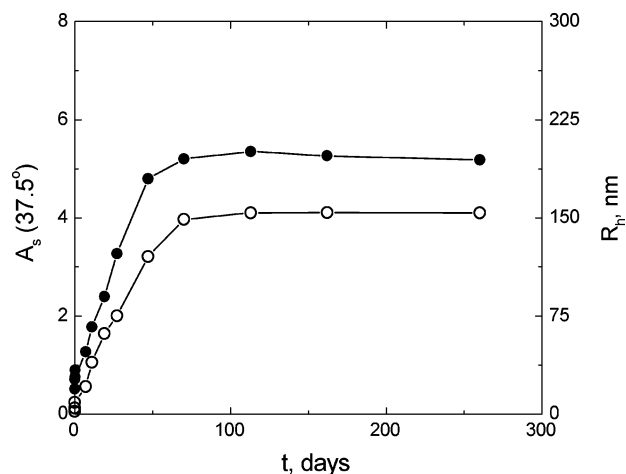


**Figure 2.** Kinetics of the domain formation in the mixture of dimethyl sulfoxide and water (10.5 mass % of DMSO). Time dependence of scattering from domains at scattering angle  $\theta = 37.5^\circ$  (○), and hydrodynamic radius of domains  $R_h$  (●). Hydrodynamic radii were calculated from diffusion coefficients extrapolated to zero scattering angle.

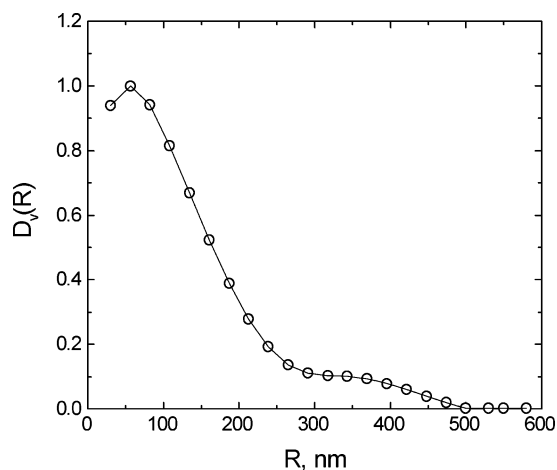


**Figure 3.** Volume size distribution of domains obtained by ORT analysis<sup>11,12</sup> of the angular dependence of scattering from domains. Data are related to the sample described in Figures 1 and 2 and was taken 260 days after mixing.

radii of domains  $R_h$ , which were calculated from diffusion coefficient  $D_s$  ascribed to domain diffusion and extrapolated to zero scattering angle. The growth of domains has a saturation character, i.e., it is faster at the beginning and then gradually slows down. The total duration of the growth is approximately 80 days. Then domains appear stable (monitored over next 170 days). Figure 3 shows domain volume size distribution  $D_v(R)$  calculated from angular dependence  $A_s(\theta)$  obtained on the mixture after 260 days (steady state). Volume size distribution of particle sizes  $D_v(R)$  means that  $D_v(R) dR$  represents the volume fraction of particles with radius from the interval  $(R, R+dR)$ . A relatively high degree of polydispersity can be seen in the size distribution. Domain sizes span from ca. 30 nm to almost 500 nm while volume fraction decreases with increasing  $R$ . The distribution function for  $R < 30$  nm cannot be calculated from light scattering data due to insufficient  $q$ -range. Therefore, it is impossible to make a conclusion from light scattering data whether the distribution function goes steeply to zero below  $R = 30$  nm or persists at higher  $D_v(R)$  values until very low  $R$ . The latter case would mean that there is also a large number of very small domains in solution which could in principle approach even solute dimers, trimers, etc. The hydrodynamic

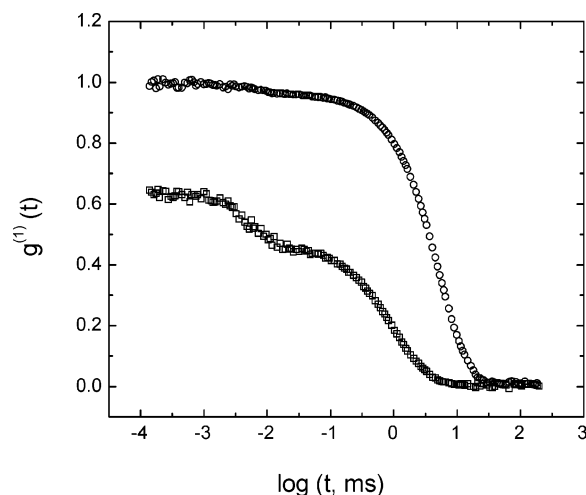


**Figure 4.** Examples of time autocorrelation functions of the electric field of scattered light  $g^{(1)}(t)$  obtained on the sample from Figures 1–3: (□) 150 min after mixing, and (○) 260 days after mixing. Autocorrelation functions are bimodal. The slower mode appears due to the presence of large domains (clusters) and gradually dominates the correlation curve. Scattering angle  $\theta = 45^\circ$ .

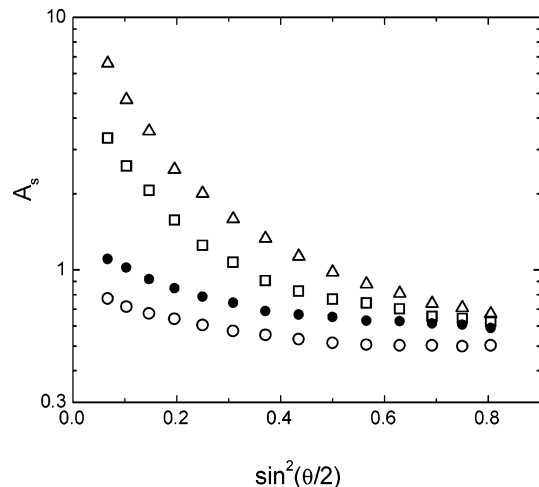


**Figure 5.** Kinetics of the formation of supramolecular domains in the mixture of ethanol and water (20 mass % of ethanol). Angular dependencies of scattering from domains were taken 1 h (○), 4 days (●), 16 days (□), and 143 days (△) after mixing.

radius  $R_h$  as shown in Figure 2 is proportional to an average size of the broad size distribution. Examples of normalized time autocorrelation functions of the electric field of scattered light  $g^{(1)}(t)$  (from which  $D_s$  and  $R_h$  are calculated) are shown in Figure 4. Autocorrelation functions are bimodal. The slower mode appears due to the presence of domains and gradually dominates over the faster mode representing classical mutual diffusion of mixture components. More details on  $R_h$  and dynamic light scattering data in general can be found in the previous paper of this series.<sup>1</sup>

Figures 5 and 6 show kinetics of the domain formation in a mixture of ethanol and water (20 mass % of ethanol). The main features of this process are very similar to what was observed in the DMSO–water mixture. Domain growth has a saturation character on a similar time scale. It results also in a similar size of domains as deduced from  $R_h$  and in a similar size distribution as deduced from angular dependencies. We will omit size distributions in the following paragraphs and will focus on raw data of angular dependencies of scattering from domains since these data contain more complex information. The

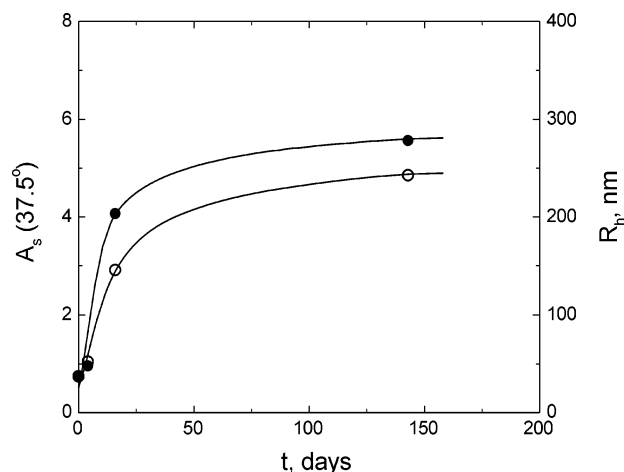


**Figure 6.** Kinetics of the domain formation in the mixture of ethanol and water (20 mass % of ethanol). Time dependence of scattering from domains at scattering angle  $\theta = 37.5^\circ$  (○), and hydrodynamic radius of domains  $R_h$  (●). Hydrodynamic radii were calculated from diffusion coefficients extrapolated to zero scattering angle.

following rules apply to its semiquantitative interpretation. Linear dependence of  $A_s$  vs  $\sin^2(\theta/2)$  corresponds to monodisperse (or narrow size distribution) domains, the slope is proportional to the domain size, and the curvature (departure from linearity) is proportional to the width of the size distribution. Absolute values of scattering amplitudes (vertical positioning of curves with given shape in plots) are proportional to the number of domains per unit volume and/or the scattering contrast (the difference of the solute concentration inside and outside the domain), i.e., to the strength of the domain effect.

An example of a relatively fast domain growth is documented in Figures 7A and 7B. Figure 7A shows real-time monitoring of the domain formation via real-time monitoring of scattering intensity after mixing two components of the mixture. Acetic acid was mixed with water (6 mass % of acid). Acid and water were separately dropped through  $0.2 \mu\text{m}$  filters directly into the scattering cell, the mixture was gently shaken for several seconds to allow for macroscopic mixing, inserted into a light scattering spectrometer, and then the measurement started. The scattering intensity of a 6% aqueous solution of acetic acid with homogeneously dispersed solute molecules (or dimers in the case of acetic acid) is expected somewhere between 0.10 and 0.15 (in units of benzene scattering). A gradual increase of scattering intensity far above this value is due to the supramolecular domain formation. In addition to the overall increase of scattering intensity, an increase of intensity fluctuations due to the presence of large scattering objects is evident. An apparent saturation of scattering intensity is observed approximately 40 min after the mixing. The total scattering is then completely dominated by the scattering contribution from domains (i.e.,  $I/I_B \approx A_s$ ). Figure 7B shows real-time monitoring of scattering from pure (unmixed) components: deionized water with time-average intensity  $I/I_B = 0.1$  and acetic acid with time-average intensity  $I/I_B = 0.44$ . These records can be considered as “blank experiments” showing that the effect is really due to mixing. They are also instructional with respect to the presentation of the purity of our samples (records show correct absolute values of intensities of pure liquids and are without any spikes that can be produced by a movement of dust or other impurity through the scattering volume). An important conclusion from the monitoring of the domain formation is that domains are not due to incomplete macroscopic or mesoscopic mixing of the components of the mixture in the beginning. Complete mixing

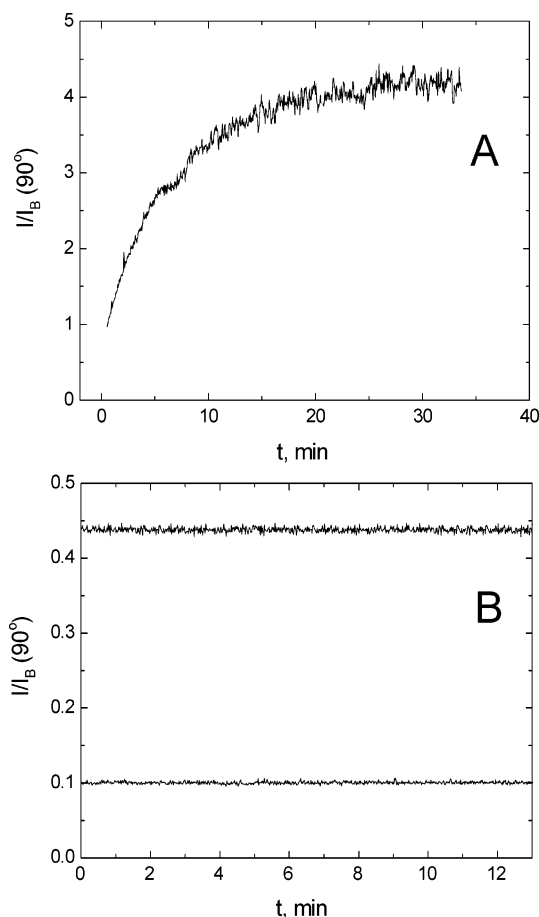


**Figure 7.** (A) Real-time monitoring of scattering after mixing two components of the mixture. Acetic acid was mixed with water (6 mass % of acid). A pronounced increase of scattering is due to the formation of domains. Scattering intensities normalized to benzene scattering were obtained by photon counting. Counts measured within consecutive time intervals of 2.35 s are plotted. In addition to the overall increase of scattering intensity, a gradual increase of intensity fluctuations due to the growth of large scattering objects is evident. (B) Real-time monitoring of scattering from pure (unmixed) components: deionized water with time average intensity  $I/I_B = 0.10$  and acetic acid with time-average intensity  $I/I_B = 0.44$ .

on the molecular level occurs first and results in very low scattering. Only then are supramolecular domains *spontaneously* formed.

A special type of kinetics of the domain formation was found in the mixture of glycerol and water (Figure 8). The mixture was monitored after mixing in intervals of several hours. No indication of the domain structure was seen. Scattering intensity stayed low and without any signature of an angular dependence. Then, after some delay of ca. 24 h, the domain structure was formed in an abrupt manner (almost in a “step-function manner”) resulting in a sudden dramatic increase of intensity and a pronounced angular dependence. Blank experiments were performed in parallel. Pure glycerol as well as pure water measured at the same conditions did not exhibit any temporal changes, confirming that the observed effect was due to mixing. The experiment described in Figure 8 was semiquantitatively reproduced four times in four separate kinetic experiments. Such kinetics indicates that that some critical conditions must be met to nucleate the process of the domain growth, which is then very rapid. The domain structure is then stable over longer time intervals. As mentioned in the first paper<sup>1</sup> of this series, some formal similarities can be found between the inhomogeneous solute distribution reported in this work and the inhomogeneous



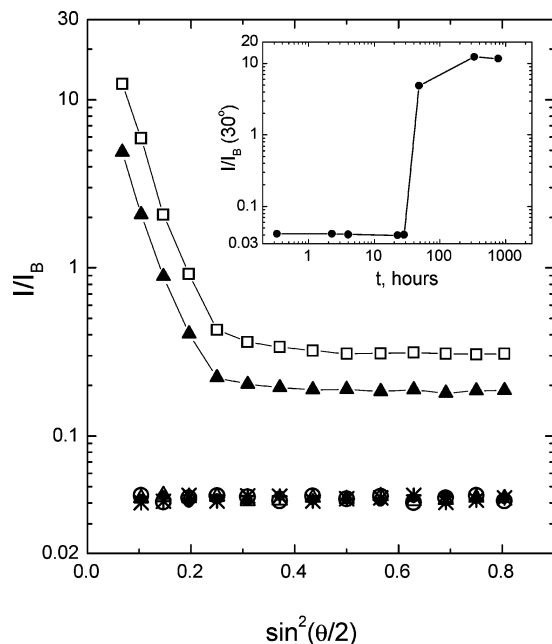


**Figure 8.** Kinetics of the domain formation in the mixture of glycerol and water (5 mass % of glycerol). Angular dependencies of scattering intensities were taken 20 min (○), 2 h (●), 4 h (\*), 22.5 h (Δ), 2 days (▲), and 14 days (□) after the sample preparation. Inset shows time dependence of scattering intensity at scattering angle  $\theta = 30^\circ$  and documents an abrupt increase of intensity due to the domain formation. Scattering intensities are net intensities corresponding to compositional fluctuations and are normalized to benzene scattering.

solution structure found in solutions of ionic polymers<sup>3–7,13–16</sup> (although the nature of attractive interaction giving rise to clustering can be different in these two cases). Regarding kinetic experiments, fast kinetics very similar to what is presented in Figure 7A was reported for ionic polymers.<sup>7</sup> Examples of slower growth of domains (similar to Figures 1–6) can be found, too.<sup>6</sup> Even the very special type of kinetics (abrupt appearance, Figure 8) was found in polymeric solutions, too.<sup>6</sup> A very slow process of association was found also in aqueous solutions of fully hydrophilic inorganic  $\{\text{Mo}_{72}\text{Fe}_{30}\}$  large anions.<sup>17,18</sup>

Kinetics of the domain formation in solutions of inorganic salts (electrolyte solutions) will be presented next. In the case of solid samples, it is not possible to monitor the very early stages of the domain formation as in the case of liquid mixtures since it is necessary to let solid samples to dissolve completely. All samples in the experiments described below were left to dissolve completely. The full dissolution was assured not only macroscopically by visual observation, but also by vapor pressure osmometry, which is sensitive to the concentration of free ions in solution. Figure 9 shows the process of the domain growth in aqueous solution of  $\text{Na}_2\text{SO}_3 \times 7\text{H}_2\text{O}$  ( $c = 4.5$  mass %) starting at  $t = 70$  min from the sample preparation. Domains are already present at this time and grow within the next ca. 50 days. When the growth of domains is completed, the size distribution does not change (the shape of  $A_s(\theta)$  is constant), however, the absolute value of  $A_s$  decreases. This is a relatively surprising scenario, which we will discuss in more detail later and will show that the decrease of  $A_s$  means that the density of domains decreases. Compared to other solutions of inorganic salts, the process of the domain growth in aqueous solution of  $\text{Na}_2\text{SO}_3$  is relatively slow. The stage of the domain growth in solutions of inorganic salts is typically much shorter, on the order of minutes or hours. Figures 10 and 11 show kinetics of the domain structure in 3M aqueous solution of  $\text{NaCl}$  ( $c = 14.5$  mass %). The stage of the domain growth is here also slightly

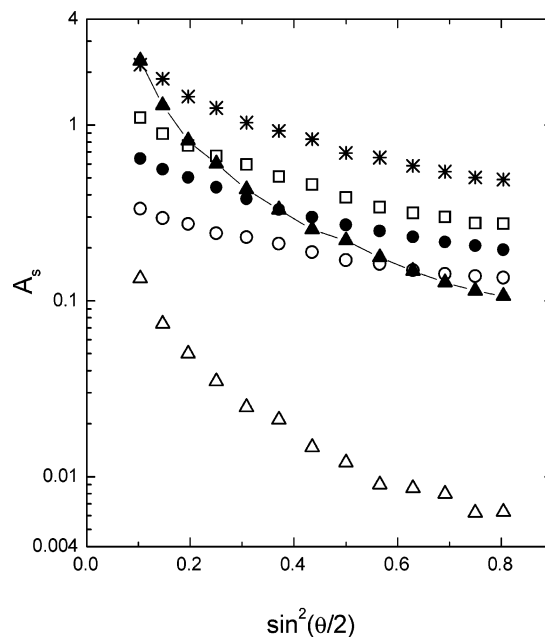


**Figure 9.** Angular dependencies of scattering from domains in aqueous solution of  $\text{Na}_2\text{SO}_3 \times 7\text{H}_2\text{O}$ ,  $c = 4.5$  mass %. Data were taken 70 min (○), 6 days (●), 13 days (□), 27 days (\*), 52 days (▲), and 108 days (Δ) after the sample preparation.

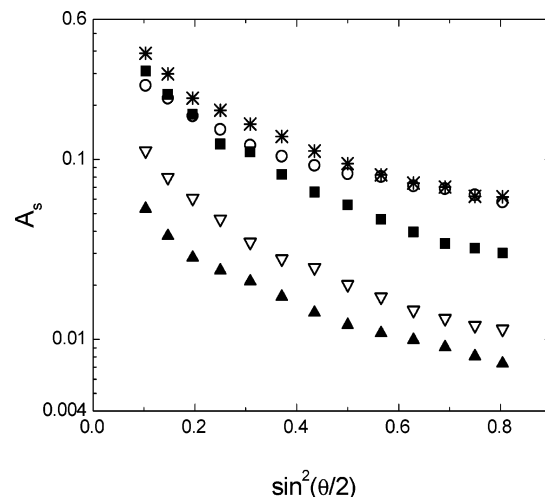


**Figure 10.** Angular dependencies of scattering from domains in 3 M aqueous solution of  $\text{NaCl}$  ( $c = 14.5$  mass %). Data were taken 30 min (○), 8 h (\*), 4 days (■), 10 days (▽), and 17 days (▲) after the sample preparation.

higher than average, approximately 4 days. Then domains persist again for quite a long time with constant size distribution (constant angular dependence of  $A_s$ ), but with a very slow continuous decrease of domain density (decrease of absolute value of  $A_s$ ). A complete fading of domains (equalization of concentrations inside and outside the domain) occurs sometime between 50 and 100 days as deduced from the asymptotic ceasing of the  $A_s$  scattering signal. Table 1 shows kinetic data on aqueous solutions of  $\text{MgSO}_4$  and  $\text{Al}(\text{NO}_3)_3$ . The stage of the domain growth is here very short, domains form almost immediately. Then a gradual decrease of the density of domains is seen while domain size distributions do not change. The decrease is such that a strong fall is observed in the beginning, with partial leveling off at longer times. Domains persist in solution almost one year after the solution preparation. Most probably, the overall trend here is also a complete equalization of local concentrations inside and outside domains. However,

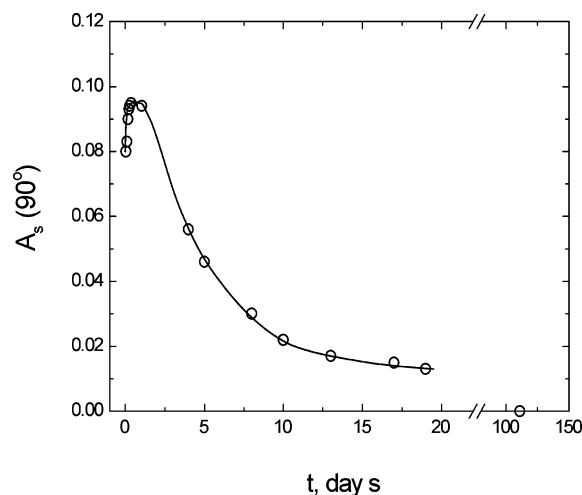


**Figure 11.** Time dependence of scattering from domains in 3 M aqueous solution of NaCl ( $c = 14.5$  mass %). The sample was the same as in Figure 10.

**TABLE 1: Time Dependence of Light Scattering Data from 0.4 M Aqueous Solutions of  $\text{MgSO}_4 \times 7\text{H}_2\text{O}$  and  $\text{Al}(\text{NO}_3)_3 \times 9\text{H}_2\text{O}$ <sup>a</sup>**

$t$ , days	$\text{MgSO}_4 \times 7\text{H}_2\text{O}$		$\text{Al}(\text{NO}_3)_3 \times 9\text{H}_2\text{O}$	
	$A_s(45^\circ)$	$A_s(90^\circ)$	$A_s(45^\circ)$	$A_s(90^\circ)$
0	12.1	2.02	1.41	0.63
0.13	-	-	0.64	0.29
6	5.24	1.05	0.31	0.16
28	2.37	0.60	0.18	0.099
51	1.08	0.29	0.11	0.056
87	0.46	0.10	0.083	0.042
184	0.29	0.058	0.058	0.031
331	0.13	0.030	0.053	0.029

<sup>a</sup>  $A_s$  is the scattering contribution from domains and is expressed in units of the scattering intensity of a benzene standard. Values at scattering angles  $\theta = 45^\circ$  and  $\theta = 90^\circ$  are shown. The ratio  $A_s(45^\circ)/A_s(90^\circ)$  reflects the steepness of the angular dependence of  $A_s$  and is proportional to average domain size. In both cases this ratio does not change with time within experimental scatter. Data indicate an extremely slow gradual decrease of domain density while the size of domains remains constant.

this may take a much longer time. It seems that the overall trend in solutions of electrolytes is that the domain structure finally ceases and the final equilibrium situation may be considered as without domains. However, solutions of electrolytes in “finite times” (as we know them and use them) exhibit a pronounced supramolecular structuring.

Now we return back to a more detailed discussion on the above-mentioned slow process of decreasing of scattering contribution from domains  $A_s$ . To realize what kind of a slow process it is, we recall that intensity of scattering at a fixed shape of the particle size distribution is given by a combination of two quantities: total number of scattering particles and scattering contrast of particles. Since it is physically very unrealistic that the number of domains would decrease with time without any changes in the shape of the size distribution, the plausible explanation is that the scattering contrast of domains gradually decreases (the difference between the solute concentration inside and outside the domain decreases). Domains become progressively looser and looser. It is necessary to note that the two kinetic processes observed, which are reflected in an increase and a subsequent decrease of scattering intensity, are not mirror-reversed processes. The first process means growth in size while the other one does not mean a reverse shrinkage. It would be strange if a spontaneously driven process

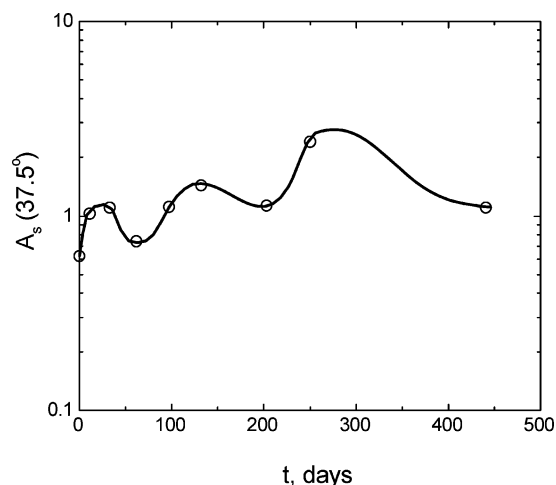


**Figure 12.** Time dependence of scattering from supramolecular domains in aqueous solution of D-glucose ( $c = 0.9$  mass %). Periodic changes in intensity (long-time oscillations) exceed significantly experimental resolution. The error bar is on the order of the symbol size.

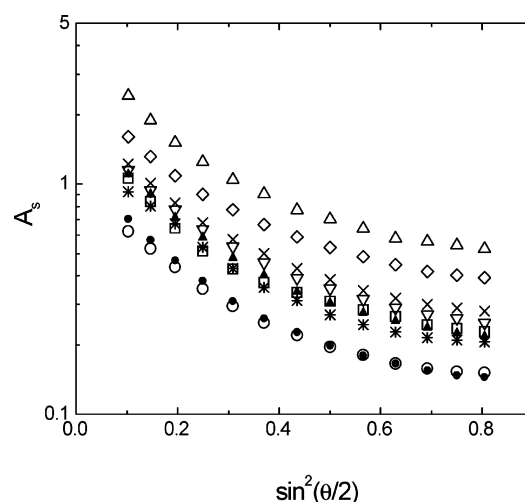


**Figure 13.** Angular dependencies of scattering from domains in aqueous solution of D-glucose ( $c = 0.9$  mass %). Data were taken 0 days (○), 11 days (\*), 33 days (▲), 62 days (●), 97 days (▽), 132 days (◇), 203 days (×), 250 days (△), and 441 days (□) after the sample preparation.

would be mirror-reversed. The two processes differ also in orders of magnitude different time scale. An analogous situation was found previously in solutions of ionic polymers, where growth of relatively dense domains on a short time scale is followed by a very slow decrease of domain density at fixed domain sizes.<sup>6,7</sup>

In contrast to solutions of electrolytes, a long-time persisting and relatively stable domain structure was found not only in liquid mixtures discussed at the beginning of this paper but also in solutions of some nonionic solid compounds, e.g., glucose and urea. Figure 12 shows long-time dependence of scattering from domains in aqueous solution of D-glucose ( $c = 0.9$  mass %). No tendency toward ceasing of the domain structure is observed up to 450 days. An interesting feature here is that periodic changes in intensity (long-time oscillations) are present. These oscillations exceed significantly experimental resolution. The error bar is on the order of the symbol size. Figure 13 shows in more detail what these oscillations mean. The size distribution of domains is practically constant (constant shape of angular dependencies of scattering), and hence the oscillations in

scattering intensity are due to slow oscillatory changes in the density of domains. This means a slow exchange of solute molecules between domains and surrounding matrix. Solvent molecules naturally replace solute molecules in domains. This is in agreement with the characterization of domains as loose structures with solvent inside.<sup>1</sup> Another argument supporting conclusion that there must be solvent inside domains (at least after some time from the sample preparation) follows from data presented in Figures 9 and 10 and in Table 1. Domain density decreases while the size remains constant. Solvent molecules simply replace solute in domains.

## Conclusions

Kinetics of the formation of large-scale supramolecular structures and their long-time stability were studied in detail in solutions of electrolytes, nonelectrolytes, and mixtures of liquids. In the case of mixtures of liquids, a complete real-time monitoring of the supramolecular structure formation was possible in all cases. Liquids were well miscible, a homogeneous mixing was achieved after several seconds of agitation. Mixtures were then continuously monitored by light scattering. The time scale on which the supramolecular structure developed varied from minutes to weeks, depending on the concrete mixture. The growth of supramolecular domains was reflected in an increase of absolute values of scattering intensity from domains, in the steepening of angular profiles of scattering, and in an increase of hydrodynamic radii obtained from dynamic light scattering data. The growth of domains was in most cases also accompanied by broadening of their size distribution. An important conclusion from the monitoring of the domain formation is that supramolecular domains are not due to incomplete macroscopic or mesoscopic mixing of the components of the mixture in the beginning. A complete mixing on the molecular level occurs first. An interesting effect was observed in mixtures of glycerol with water, where the supramolecular structure was formed in a quite abrupt manner (not continuously). Blank experiments with unmixed components were performed to ensure that the observed kinetic effects in liquid mixtures are really due to mixing.

In the case of solutions of solid samples, monitoring of the formation of supramolecular structure was possible in cases when the structure formation was significantly slower than the dissolution process itself. Complete dissolution was checked not only visually, but also by vapor pressure osmometry. Similarly

to the case of liquid mixtures, domain growth was usually accompanied by broadening of the size distribution.

The long-time stability of supramolecular domain structure was investigated in time intervals ranging up to 15 months. In some systems the resulting domain structure appeared stable. In other systems a very slow process of domains fading-out was observed. This process can be described as a very slow equalization of solute concentration inside and outside domains while the domain size distribution remains constant. An interesting feature found in a few cases was the presence of periodic changes in domain density (long-time oscillations) due to exchange of solute between domains and surrounding matrix (rest of solution). In conclusion, slow kinetic effects regarding the large-scale supramolecular structure are present in the systems investigated. Among others, data on some common substances of great chemical and biological importance such as sodium chloride, acetic acid, glucose, and ethanol, were presented.

**Acknowledgment.** Support from the Presidium of the Slovak Academy of Sciences (grant No. 2/8001/22) and from the Slovak grant agency VEGA (grant No. 2/2085/2002) is acknowledged. The author is also thankful to E. Gyöngyösiová for excellent technical assistance in experiments.

## References and Notes

- (1) Sedláč, M. *J. Phys. Chem. B* **2006**, *110*, 4329.
- (2) Schmitz, K. S. *An Introduction to Dynamic Light Scattering by Macromolecules*; Academic Press: San Diego, 1990.
- (3) Schmitz, K. S. *Macroions in Solution and Colloidal Suspension*; VCH: New York, 1993.
- (4) Sedláč, M. In *Light Scattering. Principles and Development*; Clarendon: Oxford, 1996; Ch. 4, pp 120–165.
- (5) Sedláč, M. *J. Chem. Phys.* **2002**, *116*, 5246.
- (6) Sedláč, M. *J. Chem. Phys.* **2002**, *116*, 5256.
- (7) Sedláč, M. *J. Chem. Phys.* **2005**, *122*, 151102.
- (8) Provencher, S. W. *Comput. Phys. Commun.* **1982**, *27*, 213.
- (9) Jakeš, J. *Czech. J. Phys.* **1988**, *38*, 1305.
- (10) Štěpánek, P. In *Dynamic Light Scattering. The Method and Some Applications*; Clarendon: Oxford, 1993; Ch. 4, pp 177–240.
- (11) Schnablegger, H.; Glatter, O. *Appl. Optics* **1991**, *30*, 4889.
- (12) Glatter, O.; Hofer, M. *J. Colloid Interface Sci.* **1988**, *122*, 496.
- (13) Lin, S. C.; Lee, W. I.; Schurr, J. M. *Biopolymers* **1978**, *17*, 1041.
- (14) Ermi, B. D.; Amis, E. J. *Macromolecules* **1996**, *29*, 2701.
- (15) Tanahatoe, J. J.; Kuil, M. E. *J. Phys. Chem. B* **1997**, *101*, 5905.
- (16) Matsuoka, H.; Ogura, Y.; Yamaoka, H. *J. Chem. Phys.* **1998**, *109*, 122.
- (17) Liu, T. *J. Am. Chem. Soc.* **2003**, *125*, 312.
- (18) Liu, T. *J. Am. Chem. Soc.* **2005**, *127*, 6942.